Spatial variation of microtexture in linear friction welded Ti-6Al-4V

Guo, Yina; Attallah, Moataz M.; Chiu, Yulung; Li, Hangyue; Bray, Simon; Bowen, Paul

DOI:
10.1016/j.matchar.2017.03.019

Document Version
Peer reviewed version

Citation for published version (Harvard):
Guo, Y, Attallah, MM, Chiu, Y, Li, H, Bray, S & Bowen, P 2017, 'Spatial variation of microtexture in linear friction welded Ti-6Al-4V', *Materials Characterization*, vol. 127, pp. 342-347.
https://doi.org/10.1016/j.matchar.2017.03.019

Spatial variation of microtexture in linear friction welded Ti-6Al-4V

Yina Guo, Moataz M. Attallah, Yulung Chiu, Hangyue Li, Simon Bray, Paul Bowen

PII: S1044-5803(17)30745-3
DOI: doi: 10.1016/j.matchar.2017.03.019
Reference: MTL 8599

To appear in: *Materials Characterization*

Received date: 26 July 2016
Accepted date: 12 March 2017

Please cite this article as: Yina Guo, Moataz M. Attallah, Yulung Chiu, Hangyue Li, Simon Bray, Paul Bowen , Spatial variation of microtexture in linear friction welded Ti-6Al-4V. The address for the corresponding author was captured as affiliation for all authors. Please check if appropriate. Mtl(2017), doi: 10.1016/j.matchar.2017.03.019

Spatial Variation of Microtexture in Linear Friction Welded Ti-6Al-4V

Yina Guo[a1], Moataz M. Attallah[a],Yulung Chiu[a], Hangyue Li[a], Simon Bray[b], Paul Bowen[a]

[a]School of Metallurgy and Materials, University of Birmingham, Birmingham, B15 2TT, UK.
[b]Rolls-Royce plc, PO Box31, Derby DE24 8BJ, UK

Dr. Yina Guo, Postdoctoral Researcher in Electron Microscopy, Materials & Surface Science Institute (MSSI), University of Limerick, Limerick, Ireland, Tel: (+353) (0) 6123 4627, Fax: (+353) (0) 61213529. Email: yina.guo@ul.ie

Professor Moataz Attallah, Professor of Advanced Materials Processing, School of Metallurgy and Materials, The University of Birmingham, Birmingham, B15 2TT, Tel: (+44) (0) 121 414 7842. Email: m.m.attallah@bham.ac.uk

Dr. Yu Lung Chiu, Lecturer in Electron microscopy, School of Metallurgy and Materials, The University of Birmingham, Birmingham, B15 2TT, Tel: (+44) (0) 121 414 5190
Email: y.chiu@bham.ac.uk

Dr. Hangyue Li, Senior research fellow, School of Metallurgy and Materials, The University of Birmingham, Birmingham, B15 2TT, Email: h.y.li.1@bham.ac.uk

Dr. Simon Bray, Engineering Specialist - Solid State Welding, Materials Design Service Rolls-Royce Plc, Derby DE24 8EG, Tel: +44 (0) 1332 2 40619,
Email: simon.bray@rolls-royce.com

Professor Paul Bowen, Head of School of Metallurgy, School of Metallurgy and Materials
The University of Birmingham, Birmingham, B15 2TT, Tel: (+44) (0) 121 414 5222
Email: bowenp@bham.ac.uk

ABSTRACT

The variation of microstructure and microtexture across a Ti-6Al-4V (Ti64) linear friction weld was investigated using scanning electron microscopy (SEM) and electron backscattered diffraction (EBSD). Pole figures and misorientations distribution obtained from α phase show four distinct regions within the weld, with different textural characteristics. Nevertheless, the main texture components remain the same in centre weld zone and thermal mechanical affected zone with the basal poles of the α phases located at around 0°, 60° and 90° to the sample normal (Z_0) direction. The results indicate that the texture components are strongly related to the amount of transformed β phase. The deformation of the primary α grains has a limited effect on the texture development.

[1]Materials and Surface Science Institute, University of Limerick, Ireland (This is the current address of the first author, the work presented here was done in the University of Birmingham)

Spatial Variation of Microtexture in Linear Friction Welded Ti-6Al-4V

Yina Guo[a2], Moataz M. Attallah[a], Yulung Chiu[a], Hangyue Li[a], Simon Bray[b], Paul Bowen[a]

[a]School of Metallurgy and Materials, University of Birmingham, Birmingham, B15 2TT, UK.

[b]Rolls-Royce plc, PO Box31, Derby DE24 8BJ, UK

ABSTRACT

The variation of microstructure and microtexture across a Ti-6Al-4V (Ti64) linear friction weld was investigated using scanning electron microscopy (SEM) and electron backscattered diffraction (EBSD). Pole figures and misorientations distribution obtained from α phase show four distinct regions within the weld, with different textural characteristics. Nevertheless, the main texture components remain the same in centre weld zone and thermal mechanical affected zone with the basal poles of the α phases located at around 0°, 60° and 90° to the sample normal (Z_0) direction. The results indicate that the texture components are strongly related to the amount of transformed β phase. The deformation of the primary α grains has a limited effect on the texture development.

KEYWORDS: Linear Friction Welding; Titanium Alloys; Microstructure; Electron Backscattered Diffraction (EBSD)

1. Introduction

Linear Friction Welding (LFW) is a solid-state joining method that utilises friction-induced

[2]Materials and Surface Science Institute, University of Limerick, Ireland (This is the current address of the first author, the work presented here was done in the University of Birmingham)

thermo-mechanical deformation to create high quality welds [1]. In this technique, the two components to be welded are placed in contact under a forging force, with one of the components oscillating and the other held stationary, generating sufficient heat to weld the samples together [2]. The increasing interest in the use of LFW in joining Ti-alloy components in the aerospace sector is due to the high integrity of the joint and the associated cost-efficiency of the process. A considerable amount of work on LFW of Ti-alloys, mostly Ti64, has been done to investigate the microstructural, texture, and residual stress development [3-6]. It has been suggested that the weld is divided into four zones (although different terminologies are used), namely the unaffected parent material (PM), the heat affected zone (HAZ), the thermo-mechanically affected zone (TMAZ) and the centre weld zone (CWZ) [3, 7]. Previous studies that investigated the influence of the process parameters on the microtexture development in welds of Ti-alloys have been mainly focused on the microstructure, texture and mechanical properties near the CWZ. Karadge *et al.* [3, 8] and Dalgaard *et al.* [7] showed that the welds exhibit a strong α phase texture in the TMAZ close to the CWZ, where the basal poles of the α crystallites are predominantly orientated perpendicular to both the axial force direction and the oscillation direction. Corzo *et al.* [9] studied the fracture behaviour of linear friction welded Ti6246 alloy, it was found that in most of the cases crack turns to deviate towards the HAZ. This phenomenon may relate to the microstructure and microtexture change in different zones. In order to gain a better understanding of the properties of LFW samples, it is necessary to investigate the variation of microtexture across the whole weld, which is the subject of the present study.

2. Experimental procedure

Linear friction welds of $\alpha+\beta$ - processed Ti64 alloy were received in the as-welded condition. The size of the weld is 20 mm (in the axial force direction) × 23mm (in the oscillation

direction) × 250mm. The specimens were sectioned parallel to the plane which is defined by the oscillation direction and the forging force direction from the weld and polished for scanning electron microscopy imaging (SEM) and electron backscattered diffraction (EBSD) examination. The sample coordinate for EBSD is defined as oscillation direction (X_0-direction), the axial force direction (Y_0-direction) and the sample normal direction (Z_0-direction) as shown in Fig. 1. The samples were repeatedly polished and etched in Kroll's reagent, prior to final electropolishing in an electrolyte containing 60% methanol, 35% butanol and 5% perchloric acid (vol.) at 20 V and -30 °C. Repetitive polishing and etching were essential to improve the Kikuchi pattern quality and EBSD indexing rate.

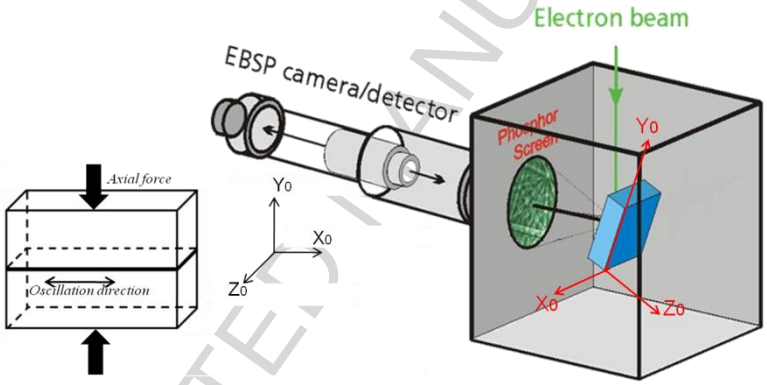

Fig. 1 Scheme of the sample geometry together with the EBSD measurement unit

EBSD maps were obtained from the middle section of the sample, covering all the different weld zones across the weld interface. A JEOL 7000 field-emission gun scanning electron microscope (FEG-SEM) equipped with INCA system, was used for the EBSD data acquisition, operating at an accelerating voltage of 20 kV, and at a working distance of 10 mm for imaging, 19 mm for EBSD mapping. The EBSD scan step size was set at ~320 nm to enable the characterisation of the fine weld microstructure. Texture analysis was performed using both INCA (for orientation map) and HKL Channel 5 (for pole figures) software due to the update of the EBSD system.

3. Results and discussion

The microstructure of the parent α+β forged Ti64 (not shown here) exhibits equiaxed α grains, with intergranular β phase. The typical microstructures of the various weld regions are shown in Fig. 2, and they generally show similar characteristics to those described in the previous study [10]. No strong texture was seen in the parent materials except some microtextured areas. In the CWZ (Fig. 2 (a)), the microstructure is entirely different from that of the PM, consisting of α′ martensite formed as a result of the rapid cooling of the dynamically recrystallized fine β grains [8]. The TMAZ microstructure shows material flow patterns associated with the reciprocating motion and the extrusion of the material during welding. In this study, the TMAZ is further divided into inner TMAZ and outer TMAZ as illustrated in Fig. 2 (b) and (c). The inner TMAZ features martensite-like α plates similar to those observed in the CWZ, but relatively finer. Residual amounts of the β phase (the brighter regions in Fig. 2 (b)), which are significantly elongated along the oscillation direction, can also be observed in this area, indicating that sub β-transus temperatures are likely to have been experienced in the TMAZ than that in the CWZ. The presence of residual β phase can be attributed to short time experienced at the near β-transus temperatures during LFW, resulting in incomplete homogenisation of the PM microstructure. Since the β-stabilisers partition to the β phase in the PM, limited time is available during LFW to allow the β-stabilisers to diffuse into the primary α grains. As a result, the areas containing high amounts of β stabilisers are retained after welding due to the fast cooling rate. In the outer TMAZ (closer to the HAZ), the martensite-like α precipitates are absent, while the elongation of the primary α grain and the retained β phase can be observed as illustrated in Fig. 2 (c). This observation suggests that the peak temperature and the high heating rate experienced during

welding may not be enough to cause a significant amount of phase transformation, but are sufficient to yield the material under the processing stresses. The microstructure of the HAZ (Fig. 2 (d)) has been only thermally affected, resulting in a 'ghost α' [11] microstructure of the PM, with no visible deformation-induced morphological changes.

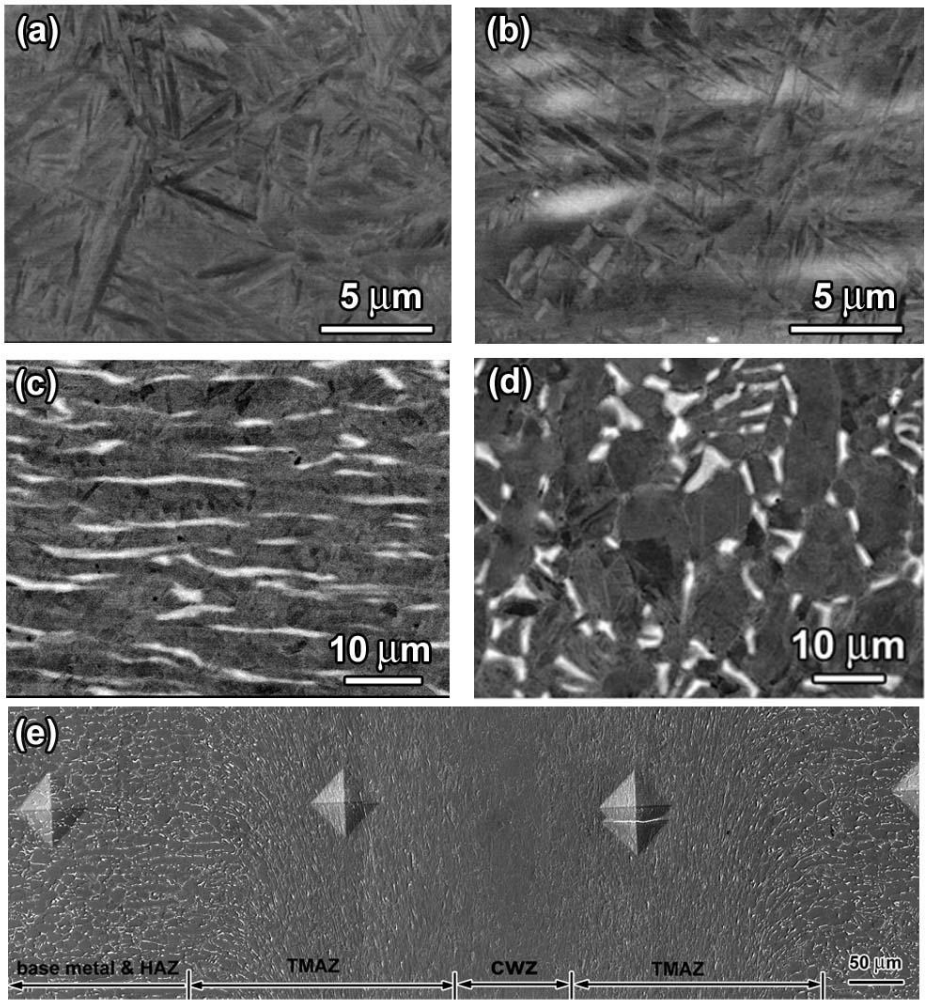

Fig. 2 Backscattered and secondary electron micrographs showing the microstructures of the different zones in the as-welded Ti64 weld. (a) CWZ; (b) inner TMAZ; (c) outer TMAZ (note that the elongated β phase which appears bright) and (d) HAZ; (e) low magnification SE micrograph showing the typical weld zones. (Note that the scale bars are different).

EBSD maps were acquired from the different weld regions. The orientation maps and the pole figures obtained from the α phase are shown in Fig. 3. It can be seen from Fig. 3 (a) and (b) that there are three dominating orientations in the Z_0-direction. The red areas in the

orientation map represent those crystals with their basal poles parallel to Z_0. The blue regions indicate that the $\{10\bar{1}0\}_\alpha$ poles of the crystals are parallel to Z_0, in other words, the basal poles of these crystals are perpendicular to Z_0. The areas in purple are the crystals with their $\{\bar{1}011\}_\alpha$ poles perpendicular to Z_0, which means that their basal poles are about 60° to Z_0. The observations are in agreement with the literature [7-10]. However, some changes can also be noticed in Fig. 3 (a), where the texture components are not as symmetrical as was reported previously [10], and the intensity of some texture components has increased significantly, especially in the inner TMAZ. This discrepancy could be caused by the fact that the EBSD maps cover a relatively small area in this study (approximately 90 μm × 60 μm). Although the CWZ is very narrow (typically less than 100 μm), microtexture characterization performed by different researchers could have been generated from different areas in the CWZ, thus leading to slight changes in the pole figures.

Fig. 3 (b) shows an EBSD map from the inner TMAZ (~70 μm from the weld centerline). As shown in Fig. 2(b), although the elongation can be observed in the retained β phase in this area, the transformed β microstructural features reveal similar characteristics to those in the CWZ. Similarly, the microtexture found in this region also shows the similarity to that in the CWZ, as demonstrated in Fig. 3(b). Although texture components similar to those identified in the CWZ were identified in the inner TMAZ pole figures, a significant intensity increase of $(0001)//Z_0$ component can be noticed, whereas the relative intensity of the components where their basal poles are about 60° to Z_0 has weakened. Also, a slight rotation of the $\{11\bar{2}0\}_\alpha$ poles can be observed in the $\{11\bar{2}0\}_\alpha$ pole figure, compared to those in the CWZ.

Fig. 3 (c) shows the EBSD results obtained at ~420 μm from the weld centreline, corresponding to the microstructure shown in Fig. 2 (c). The amount of acicular α phase

(marked with white arrow) is limited, and mainly found surrounding the retained β phase which is black in the corresponding orientation map. It can be seen from the α phase orientation map, that different orientations were observed within the elongated α grains (marked with white lines), showing that recrystallization occurred in the α phase. The $\{0001\}_\alpha$ and $\{11\bar{2}0\}_\alpha$ pole figures depict similar texture components to that shown in the inner TMAZ, but with much lower intensity. This region is likely to have experienced lower strains and temperatures, compared to the CWZ and inner TMAZ. The occurrence of α-phase recrystallization suggests that temperatures within the range ~750-900˚C were observed [12].

Fig. 3 (d) shows the EBSD results obtained from the outer TMAZ which is very close to HAZ. Again, the elongated microstructure can be seen in this area, and as it is close to HAZ, the grain sizes of the distorted primary α grains seen here are between 10 and 20 μm in length. The discrepancy of the α textures between the two different outer TMAZ regions is clearly visible from the pole figures shown in Fig. 3 (c-d). The texture components exhibited in the other weld regions such as CWZ and inner TMAZ are not visible in Fig. 3 (d). The orientations of the primary α phases retained in this region are the dominant orientations shown in the pole figures. For instance, the texture component of which its basal pole is marked in $\{0001\}_\alpha$ pole figure is related to the primary α which is in green in the orientation map. This is explains the complete change in the pole figures in the outer TMAZ.

It is of interest that the pole figures in Figures 3 (a-c) show that the textures in the CWZ and the inner TMAZ have similar characteristics. The $(0001)//Z_0$ and $<11\bar{2}0>//(X_0)$ component is about 4 to 5 times stronger than the other texture components in the CWZ and the inner TMAZ. This component is very similar to the main texture component observed in hot-rolled Ti64 [13] and the ideal P_1 shear texture of HCP materials, where the basal pole concentrates

on the shear plane perpendicular to the shear direction and one of the $\{11\bar{2}0\}_\alpha$ poles is parallel to the shear direction [14]. There exists another texture component, where its basal poles are perpendicular to Z_0, and making an angle of ~30º with the oscillation direction (X_0), which resembles the HCP shear texture C_1-fiber and C_2-fiber in which the basal pole tilts ± 30° from the shear direction towards shear plane normal [14]. Other texture components, where their basal poles are at about 60° from the Z_0 direction, are sometimes observed with very low intensity in Ti64 which was hot-rolled at β phase field [15].

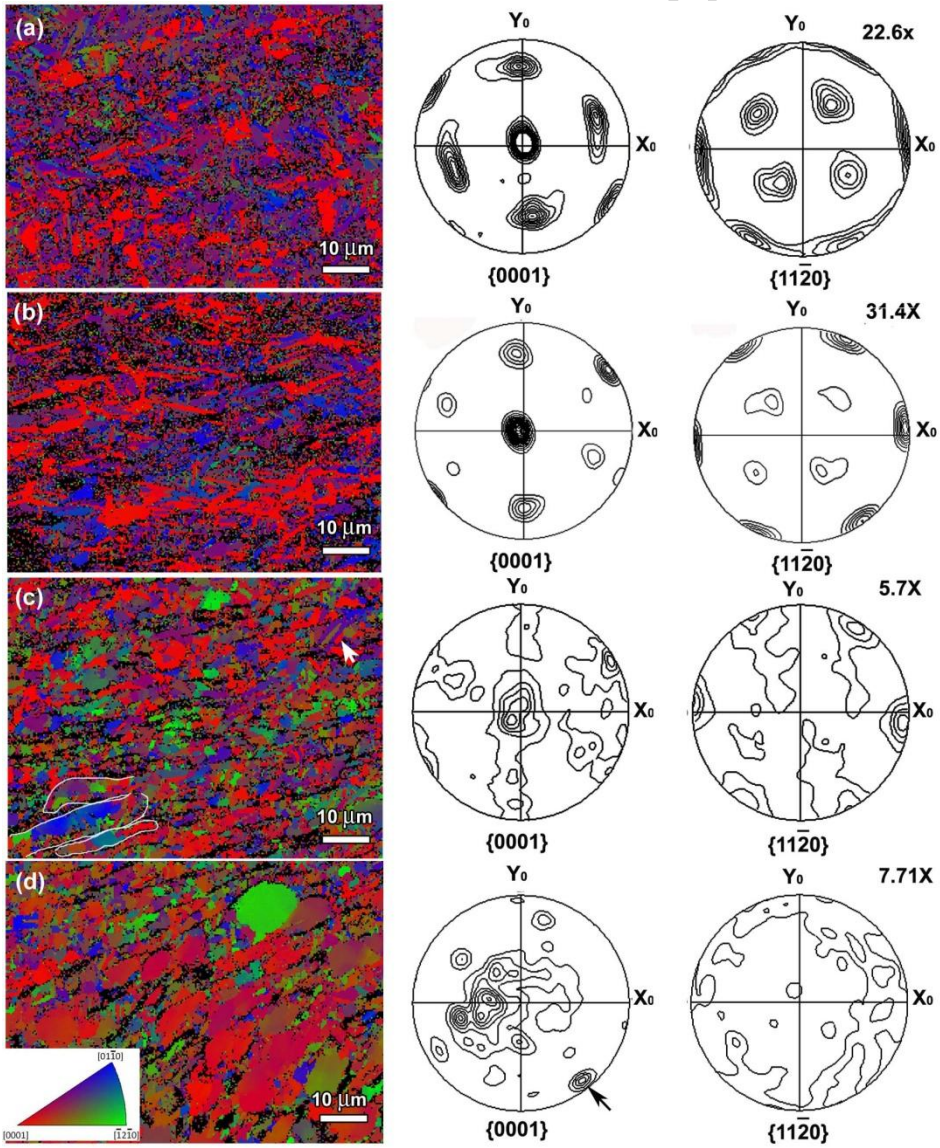

Fig. 3 EBSD results obtained in the different weld zones in as-welded Ti64 weld, showing the α phase orientation maps with respect to the sample normal direction and the {0001}α and {11$\bar{2}$0}α pole figures

of (a) CWZ; (b) inner TMAZ (70 μm from weld interface); (c) outer TMAZ (420 μm from weld interface) and (d) outer TMAZ (transition to HAZ) (d). The coordinate system, where Y0 is parallel to forging pressure direction and X0 is parallel to oscillation direction, is applied to all the images and pole figures. The contours in the pole figures from (a) to (d) show increment of 2.4, 1.9, 1 and 1 times random, respectively.

The development of the texture in linear friction welded samples can be attributed, either to the transformation texture inherited from the β phase, or to the deformation in the α phase after the phase transformation, or to both. Therefore, to understand the formation of the α texture, it is vital to know the orientation of the β phase. It is impossible to measure the β phase texture in the CWZ in as-received Ti64 LFW welds because of the martensitic transformation after welding. Previous researchers have obtained $\{110\}_\beta$ and $\{111\}_\beta$ pole figures from high resolution EBSD maps in the post weld heat treated (PWHT) LFW sample [3], and seen a similarity between the $\{0001\}_\alpha$ pole figures and $\{111\}_\beta$ pole figures. However the β phase measured was formed after the PWHT, the orientation of the high temperature β phase in the welding process remains unknown. The orientation of the high temperature $\{110\}_\beta$ pole figure was calculated from the measured α phase in the previous study [16], and it resembles the $\{0001\}_\alpha$ pole figures. In addition, a study by He *et al.* [17] shows that factors such as deformation strain, strain rate and cooling rate have no significant influence on the Burgers orientation relationship during β→α phase transformation. Therefore, it is rational to deduce that the orientation of the high temperature β grains plays an important role in the final α texture. This can possibly explain the fact that the CWZ and inner TMAZ have similar strong textures, because both regions consist of large amounts of transformed β structure. In addition, no sign of heavy plastic deformation can be observed from the morphology of the transformed β in these two regions. This suggests that the

presence of the texture components observed could be mainly attributed to the inherited α variants after the β→α phase transformation. In contrast, in the outer TMAZ, where only trace amounts of transformed β structure were seen, very weak texture was observed. This suggests that the equiaxed α grains in the outer TMAZ has little contribution to the final texture. However, detailed studies of these recrystallised α grains are necessary in the future.

The frequency-misorientation distributions of the α phase derived from different weld zones and the parent material are shown in Fig. 4. The misorientations shown here are measured between neighbouring pixels from the EBSD maps. As can be seen, despite the high frequency at low misorientation angles (<3°), the misorientation distributions are not always the same in different regions of weld. In the parent material, the misorientation angles are almost equally distributed from 10° to about 94°, with a slight increment around 60° (Fig. 4 (f)). Similar misorientation distribution has been reported in a Ti64 sample isothermally forged at 910 ºC [13]. Despite the high frequency at low misorientation angles, in the present work two other peaks, i.e. around 60° and 90°, have been observed in the CWZ and TMAZ (Figures 4 (a-d)). It should be noted that peaks at similar misorientation positions are expected from α variants transformed from a single β grain [18]. According to the Burgers orientation relationship ($\{110\}_\beta$ // $\{0001\}_\alpha$ and $<\bar{1}11>_\beta$ // $<\bar{1}2\bar{1}0>_\alpha$), when α variants are formed in a prior β grain, certain misorientation angles are generated, and the ratio of the possibilities of different misorientation angles at 10.53°, 60-63.26° and 90° can be easily calculated, and is 1:8:2 [18, 19]. In the CWZ, the frequency for misorientations at 57.9-65.1° and 88.0-90.9° is about 43.24% and 10.79%, respectively. It can be seen that the measured misorientations are almost consistent with those calculated by the Burgers orientation relationship. However, the peak at 10° has not reached up to ~5% which was expected for a random distribution of variants, indicating some α variants have not been selected during

phase transformation. This phenomenon can be explained by the effect of self-accommodation on the α/α variants selection in the martensitic transformation in Titanium proposed by Wang [18]. It was found in their study that the clusters of α variants which have misorientations around 60-63.26° accommodate most the shape strain in the diffusionless β→α transformation.

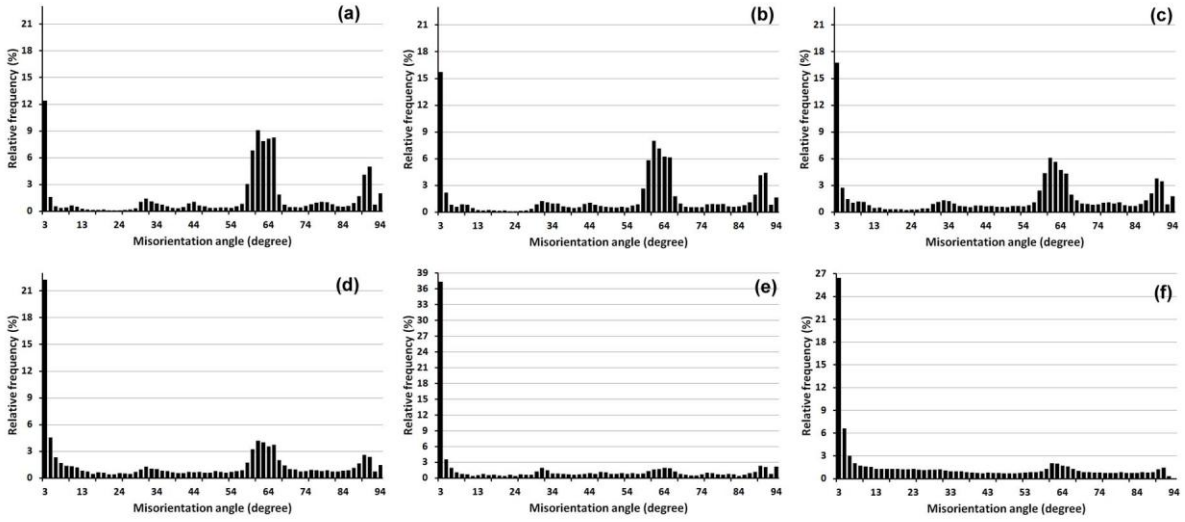

Fig. 4 Frequency-misorientation graphs of different zones. (a) CWZ, (b) inner TMAZ (70 μm from weld interface), (c) outer TMAZ (420 μm from weld interface), (d) outer TMAZ (transition to HAZ), (e) HAZ and (f) parent materials.

As can be seen from Fig. 4 (a) to (d), the frequency for misorientations of 57.9-65.1° and 88.0-90.9° decreases with the distance from the CWZ to the outer TMAZ, and the ratio between them also changes accordingly. In the HAZ (Fig. 4 (e)), the frequency at those two angle ranges is much lower, and the whole frequency-misorientation distribution is very similar to that in the parent material. In other words, the misorientations featured by the 12 α variants transformed from β become less significant from the CWZ of the HAZ because of the decrease of the amount of the transformed β phase due to the temperature gradient experienced in different zones.

In order to examine the effect of the primary α phase on the texture formation of outer TMAZ (transition zone to HAZ), comparison has been made between the pole figures obtained with and without primary α from the same EBSD map. Fig. 5 shows the α orientation maps and the $\{0001\}_\alpha$ and $\{11\bar{2}0\}_\alpha$ pole figures obtained from the transition region between the TMAZ and the HAZ in a Ti64 weld. As can be seen from Fig. 5 (a), the pole figures are different from those in the CWZ and TMAZ (c.f. Figures 3(a-b)) and do not show a very strong microtexture. However, when the primary α grains are deliberately excluded and the resulted $\{0001\}_\alpha$ and $\{11\bar{2}0\}_\alpha$ pole figures (Fig. 5 (b)) are similar to those observed in the other regions of the weld (see Fig. 3b for example). This further suggests that the primary α grains do not have significant contribution to the texture developed in the Ti64 weld. This is consistent with the observation on the above misorientation distribution analysis in different areas which suggests that the β-to-α transformation is the key in the final texture formed.

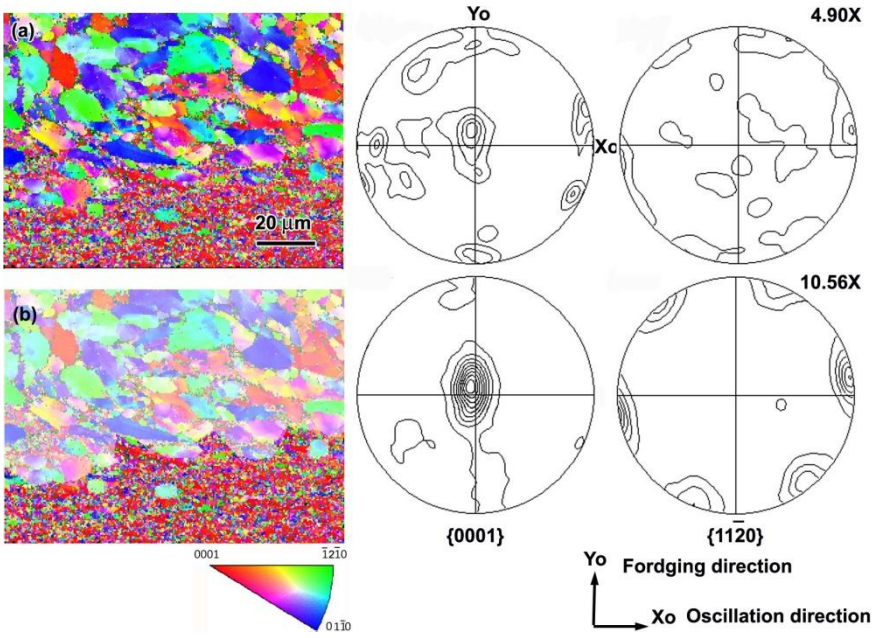

Fig. 5 EBSD results of one side of TMAZ in a Ti64 weld, (a) α phase orientation map with regard to Z0 direction with the {0001}α and {11$\bar{2}$0}α pole figures; (b) orientation map without primary α with the {0001}α and {11$\bar{2}$0}α pole figures. The contours in all pole figures show increment of 1.1 times random.

4. Conclusion

In the present paper, the microstructures and crystallographic texture distribution at different positions of as-welded linear friction welded Ti64 have been examined using SEM and EBSD. Comparisons of the microstructure, texture and misorientation distributions in different weld zones were carried out. The texture changes gradually from the CWZ to the HAZ. Nevertheless, the main texture components remain in CWZ and TMAZ are those with the basal poles of the α phases located at around 0°, 60° and 90° to the Z_0 direction. The misorientation distribution analysis indicates that the resultant texture is strongly related to the amount of transformed β in the microstructure. In the CWZ and inner TMAZ, which contain a large amount of transformed β, very strong (0001)//Z_0 texture was observed. On the contrary, in the outer TMAZ, where only the elongation of the primary α-grains was seen, the texture intensity decreased significantly, consistent with the hypothesis that the primary α grains have an insignificant effect on the texture formation in the weld.

Acknowledgement

The authors would like to thank Rolls-Royce plc for the financial support and provision of materials for the research. Discussion with Dr Rengen Ding has been gratefully acknowledged.

Reference:

1. Wanjara, P. and M. Jahazi, *Linear Friction Welding of Ti-6Al-4V: Processing, Microstructure, and Mechanical -Property Inter-Relationships.* Metallurgical and Materials Transaction A 2005. **36A**: p. 2151-2164.
2. Karadge, M., et al., *Microstructure, texture, local tensile properties and residual stress relief in Ti-6Al-4V linear friction welds* Materials Science & Technology 2006 Conference and Exhibition (MS&T Partner Societies), 2006: p. 1313-1321.
3. Karadge, M., et al., *Texture development in Ti-6Al-4V linear friction welds.* Materials Science and Engineering A, 2007. **459**(2007): p. 182-191.
4. Li, W.Y., et al., *Microstructure characterization and mechanical properties of linear friction welded Ti-6Al-4V alloy.* Advanced Engineering Materials, 2008. **10**(1-2): p. 89-92.
5. Frankel, P., et al., *Comparison of residual stresses in Ti-6Al-4V and Ti-6Al-2Sn-4Zr-2Mo linear friction welds.* Materials Science and Technology, 2009. **25**: p. 640-650.
6. Romero, J., et al., *Effect of the forging pressure on the microstructure and residual stress development in Ti-6Al-4V linear friction welds.* Acta Materialia, 2009. **57**(18): p. 5582-5592.
7. Mateo, A., et al., *Welding repair by linear friction in titanium alloys.* Materials Science and Technology, 2009. **25**: p. 905-914.
8. Dalgaard, E., et al., *Texture Evolution in Linear Friction Welded Ti-6Al-4V.* Advanced Materials Research, 2010. **THERMEC 2009 Supplement**.
9. Corzo, M., et al., *Fracture behaviour of linear friction welds in titanium alloys.* Anales de la mecanica de Fractura 2007. **1**: p. 75-80.
10. Guo, Y., et al. *Microstructure and microtexture of linear friction welded Ti-6Al-4V*. 2011.

11. Attallah, M., et al., *Microstructural and Residual Stress Development due to Inertia Friction Welding in Ti-6246.* Metallurgical and Materials Transactions A, 2012. **43**(9): p. 3149-3161.

12. Seshacharyulu, T., et al., *Hot deformation and microstructural damage mechanisms in extra-low interstitial (ELI) grade Ti–6Al–4V.* Materials Science and Engineering: A, 2000. **279**(1–2): p. 289-299.

13. Takeuchi, Y. and Y. Mae, *Influence of Rolling conditions on Texture and Mechanical properties of Ti-6Al-4V sheet.* Z. Metallkunde, 1974. **65**(11): p. 676-680.

14. Fonda, R.W. and K.E. Knipling, *Texture development in near-[alpha] Ti friction stir welds.* Acta Materialia, 2010. **58**(19): p. 6452-6463.

15. Gey, N., et al., *Modeling the transformation texture of Ti-64 sheets after rolling in the beta-field.* Materials Science and Engineering A, 1997. **230**(1-2): p. 68-74.

16. Guo, Y.N., *Microstructure and texture characterisation of linear friction welding of Ti-6Al-4V and Ti-6Al-2Sn-4Zr-6Mo*, in *School of Metallurgy and Materials*. 2012, The Univeristy of Birmingham: Birmingham. p. 274.

17. He, D., et al., *Influences of deformation strain, strain rate and cooling rate on the Burgers orientation relationship and variants morphology during $\beta \rightarrow \alpha$ phase transformation in a near α titanium alloy.* Materials Science and Engineering: A, 2012. **549**: p. 20-29.

18. Wang, S.C., M. Aindow, and M.J. Starink, *Effect of self-accommodation on alpha/alpha boundary populations in pure titanium.* Acta Materialia, 2003. **51**(9): p. 2485-2503.

19. Gey, N. and M. Humbert, *Characterization of the variant selection occurring during the α-->β-->α phase transformations of a cold rolled titanium sheet.* Acta Materialia, 2002. **50**(2): p. 277-287.